Journal of Coordination Chemistry

ISSN: 0095-8972 (Print) 1029-0389 (Online) Journal homepage: www.tandfonline.com/journals/gcoo20

A kinetic and mechanistic study of dinuclear Pt(II) 2,2':6',2"-terpyridine compounds bridged with polyethyleneglycol ether flexible linkers

A. Shaira & D. Jaganyi

To cite this article: A. Shaira & D. Jaganyi (2015) A kinetic and mechanistic study of dinuclear Pt(II) 2,2':6',2"-terpyridine compounds bridged with polyethyleneglycol ether flexible linkers, Journal of Coordination Chemistry, 68:17-18, 3013-3031, DOI: 10.1080/00958972.2015.1064114

To link to this article: https://doi.org/10.1080/00958972.2015.1064114

Journal of Coordination Chemistry, 2015
Vol. 68, Nos. 17–18, 3013–3031, http://dx.doi.org/10.1080/00958972.2015.1064114

A kinetic and mechanistic study of dinuclear Pt(II) 2,2′:6′,2″-terpyridine compounds bridged with polyethyleneglycol ether flexible linkers

A. SHAIRA and D. JAGANYI*

School of Chemistry and Physics, University of KwaZulu-Natal, Scottsville, South Africa

(*Received 9 January 2015; accepted 29 May 2015*)

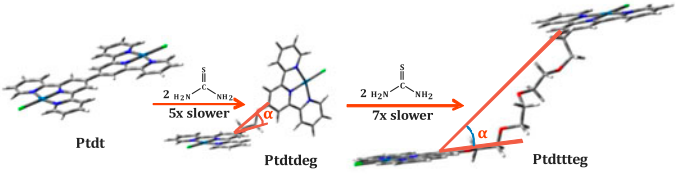

Introduction of ethyleneglycol ether linker decreases the electrophilicity of the platinum center and the whole complex. The rate of substitution reactions is controlled by both electronic and steric hindrance which increases with the length of the linker

A series of dinuclear Pt(II) complexes bridged with polyethyleneglycol ether of the type [ClPt(tpy)O$(CH_2CH_2O)_n$(tpy)PtCl]Cl_2 where n = 1 **(Ptdteg)**, 2 **(Ptdtdeg)**, 3 **(Ptdtteg)**, 4 **(Ptdttteg),** and linker-free complex, **(Ptdt)** (where tpy = 2,2′:6′,2″-terpyridine), were synthesized and characterized to investigate the role of bridging polyethyleneglycol ether linker on the substitution reactivity of dinuclear Pt(II) complexes. Substitution reactions were studied using thiourea nucleophiles, *viz*. thiourea (TU), 1,3-dimethyl-2-thiourea (DMTU), 1,1,3,3-tetramethyl-2-thiourea (TMTU) under *pseudo*-first-order conditions as a function of concentration and temperature by conventional stopped-flow reaction analyzer. The reactions gave single exponential fits following the rate law $k_{obs} = k_2$[Nu]. Introduction of polyethyleneglycol ether linker decreases the electrophilicity of the platinum center and the whole complex. The results obtained indicate that the rate of substitution is controlled by both electronic and steric hindrance which increases with the length of the linker. Experimental results are supported by density functional theory calculations and structures obtained at B3LYP/LANL2DZ level. The order of the reactivity of the nucleophiles is TU > DMTU > TMTU. The magnitude and the size of the enthalpy of activation and entropy of activation support an associative mode of mechanism, where bond formation in the transition state is favored.

Keywords: Substitution kinetics; Mechanistic study; Dinuclear platinum; Polyethyleneglycol ether; Terpyridine

*Corresponding author. Email: jaganyi@ukzn.ac.za

Introduction

Platinum metallodrugs play an important role in the treatment of cancer and modification of nucleic acids [1–5]. Multinuclear platinum complexes comprise a new class of promising anticancer agents with comparable cytotoxicity [6–14]. Compared to cisplatin, they are more water soluble and offer better DNA interactions due to their high charge [15]. Multinuclear Pt(II) complexes that can interact with DNA were first synthesized by Farrell *et al.* [11, 16–18]. The most successful of these complexes are the monodentate amine complexes $[[19]_2[19]]^{4+}$ **(BBR3464)** and $[\{trans\text{-}PtCl(NH_3)_2\}_2\{\mu\text{-}C_2H_4(NH_2(CH_2)_6NH_2)_2\}]^{4+}$ **(BBR3610)** [14, 17, 20]. The complexes show enhanced cytotoxicity against lung, pancreatic, and melanoma cancers [7]. The interaction of those complexes with DNA was found to be based on their structural–activity relationships that depend on the length of the linker and the average distance between the Pt(II) centers [6, 16, 21]. Furthermore, for dinuclear Pt(II) complexes, it was found that the reactivity of the first metal center is independent of the other [19, 22]. However, in some cases, interactions between the two Pt(II) centers have been reported [23, 24]. Therefore, data in the literature are too limited to formulate a clear relationship between the nature of the bridging ligands and the reactivity of the Pt centers [25].

Apart from the Pt···Pt distances, the nature of the linker or the spacer plays a crucial role in cytotoxicity and the reactivity of multinuclear complexes [25–27]. For example, the flexibility and hydrophilicity of the linker influence the reactivity and the cytotoxicity of the complexes in a biological environment [25]. The hydrophilicity of the linker can be increased by introducing polar groups into its linker [28]. The advantage of having a flexible linking unit over a mononuclear complex is that the linker provides variable flexibility and reduces the steric hindrance between the two monomer binding units [28]. Furthermore, hydrophilic flexible bridging linkers between two platinum centers can provide additional interactions with the proteins and the biomolecules in the body which in turn might enhance the drug carrying ability in the body [28]. For instance, in the case of **BBR3464**, one of the factors accounted for its higher activity against tumor cells was attributed to its ability to form long-range flexible intra-strand cross-links, straddling over four nucleobases of DNA [29].

2,2′:6′,2″-Terpyridine, most commonly known as tpy, and its derivatives are extensively used mostly due to their excellent photochemical and DNA intercalating properties [7, 11]. In some cases, coordinated compounds of terpyridine do not show cytotoxic behavior [30]. However, coupling of two active terpyridine moieties was found to improve this activity [26]. The ethyleneglycol ether linker increases the flexibility of the ligand so that it can wrap around DNA [26]. Previous studies have shown that a number of multinuclear complexes have been synthesized using this linker and 4′-chloroterpyridine ligand. Biological activities of such complexes have been studied using 9-ethylguanine.

DNA interaction of the dinuclear Pt(II) complex, [ClPt(dtdeg)PtCl] (where dtdeg = bis [4′-(2,2′:6′,2″-tpyridyl)]-diethyleneglycol ether), studied using Calf Thymus (CT) DNA as a substrate [26] showed a very high activity against all the cancer cell lines tested, in some cases with better activity than cisplatin [26]. Furthermore, the activity of the dinuclear complex was higher than its mononuclear complex, [Pt(tpy)Cl]Cl, indicating that the modification of the primary terpyridine ligand system improves the biological activity of the complex [26]. However, to understand this behavior of interaction with DNA, one needs to understand the mechanism of action of substitution behavior of such complexes with biological molecules.

The mechanistic understanding of how these flexible linkers control the ligand substitution behavior at the platinum centers has not been studied extensively. Recently, a number of ligand substitution reactions of dinuclear Pt(II) complexes have been reported [27, 31–35]. Studies have shown that reactivity is controlled by the distance between the platinum centers and the symmetry of the complexes [32, 33]. This increase in reactivity was attributed to an increase in charge density around the platinum center facilitated by increase in the electrostatic interactions with simultaneous reduction of the σ donation to each platinum center [33]. Reports from van Eldik *et al.* [31, 32] based on the substitution of aqua ligands from an alkyldiamine-bridged dinuclear platinum complex further support the decrease in the reactivity with the increase in the length of the flexible alkyldiamine linker. Furthermore, the results obtained showed greater reactivity for an odd number of CH_2 groups in the alkyldiamine ligand [31, 33].

In our previous work with mononuclear Pt(II) complexes, we found that the σ donacity of polyethyleneglycoxy linker reduces the π-acceptability of terpyridine. In this study, our aim was to increase our understanding of the role flexible polyethyleneglycol ether linkers on the reactivity of the dinuclear Pt(II) terpyridine complexes have when a second terpyridine group is coupled with the polyethyleneglycoxy linker. To accomplish this, we have synthesized and characterized five dinuclear Pt(II) complexes of which four complexes are linked by polyethyleneglycol ether units of different monomer units. The linker-free dinuclear complex,

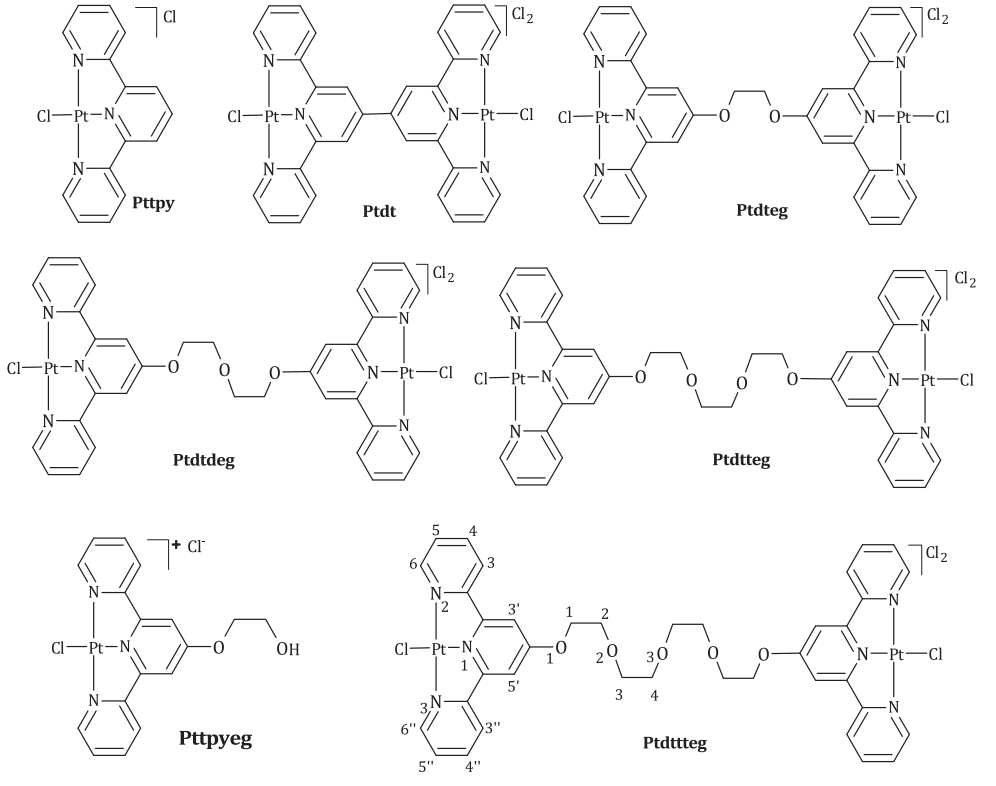

Figure 1. Structures of polyethyleneglycol ether linked dinuclear Pt(II) complexes studied. Shown on the diagram is the numbering scheme used. Pttpy is included for reference.

Ptdt, was used to gain an in-depth understanding on the role of the ethyleneglycol ether linker on controlling the reactivity of the dinuclear complexes. $[Pt(tpy)Cl]^+$ and Pt(II) (4′-(ethyleneglycoxy)-2,2′:6′,2″-terpyridine (**Pttpyeg**) from our previous work are used to compare the reactivity of the dinuclear complexes. The complexes used in this investigation are shown in figure 1.

Experimental

Materials

Methanol (Merck) was distilled over magnesium prior to use for kinetic analysis [36]. Dimethylsulfoxide (99.9%) from Aldrich was used without purification. Ethylene glycol (99.8%), diethylene glycol (99%), and triethylene glycol (99%) were bought from Sigma-Aldrich. The ligand, 4′-chloro,2,2′:6′,2″-terpyridine (97%), tetraethyleneglycol (99%), and the platinum salt, potassium tetrachloroplatinate (II) (99.9%) were bought from Aldrich. All other chemicals were purchased from Sigma-Aldrich and used without purification.

Synthesis of ligands

6′,6″-Bis(2-pyridyl)-2,2′:4′,4″:2″,2‴-quaterpyridine (dt) was synthesized following a literature method [37], and ethyleneglycol ether linked ligands are synthesized according to the literature procedure [38].

6′,6″-Bis(2-pyridyl)-2,2′:4′,4″:2″,2‴-quaterpyridine (dt) [37]

To a solution of $[Ni(PPh_3)_2Cl_2]$ (2.94 g, 4.5 mmol) and PPh_3 (2.36 g, 9 mmol) in DMF (15 mL) was added zinc dust (0.30 g, 4.5 mmol) and reaction mixture was stirred at room temperature for 30 min. The resulting red suspension was treated with 4′-chloro-2,2′:6′,2″-terpyridine (0.6 g, 4.5 mmol) which immediately changed to dark green. After stirring the reaction mixture at room temperature for 8 h, solvent was removed *in vacuo*. The residue obtained was boiled in water (50 mL) for 10 min, cooled, and filtered. The greenish brown filtrate was treated with ammoniumhexafluorophosphate (1.5 g, 9 mmol). The precipitate formed was filtered, and the solid was dissolved in a mixture of acetonitrile and water (1:4, 50 mL) and refluxed for one hour with sodium cyanide (1.5 g, 30 mmol). The yellow solid formed was filtered, washed with methanol, and dried. Recrystallization of the solid in methanol (20 mL) gave colorless needles.

Yield: 111 mg, (69%), colorless needles. The ^{1}H NMR spectra and the mass spectra are in good agreement with the proposed chemical structure. ^{1}H NMR (400 MHz, $CDCl_3$) δ/ppm[†]: 8.72 (4H, d, 6 6″), 8.61 (4H, d, 3 3″), 8.51 (4H, s, 3′ 5′), 7.88 (4H, dt, 4 4″), 7.35 (4H, dt, 5 5″). TOF MS-ES$^+$, m/e: 487.1639, $(M + Na)^+$.

[†]s = singlet, d = doublet, t = triplet, dt = doublet of a triplet. The same representation is used for the other complexes.

Synthesis of bis[4′-(2,2′:6′,2″-terpyridyl)]- ethyleneglycol ether ligands [38]

A mixture of ethyleneglycol (with variable chain lengths, *viz*. ethyleneglycol, diethyleneglycol, triethyleneglycol, and tetraethyleneglycol) with 2 equivalents of 4′-chloro-2,2′:6′,2″-terpyridine and excess KOH were stirred in dry DMSO at 60 °C for 24 h under nitrogen. After cooling the reaction mixture to room temperature, water was added, resulting in a white precipitate. The precipitate was filtered, washed with water, and air-dried. The crude product was refluxed in ethanol (98%) for half an hour. The pure product was precipitated upon cooling the mixture in ice for about 30 min. The precipitate was filtered, washed with a small amount of ice cold ethanol, and air-dried.

The purity of the ligands was confirmed using ^{1}H NMR and mass spectroscopy. The ^{1}H NMR spectra obtained show similarity in the aromatic region for the ethyleneglycol ether linked ligands.

Bis[4′-(2,2′:6′,2″-terpyridyl)]- ethyleneglycol ether (dteg). Yield: 109 mg, (54%), off-white powder. ^{1}HNMR (400 MHz, $CDCl_3$) δ/ppm: 8.72 (4H, d, 6 6″), 8.65 (4H, d, 3 3″), 8.15 (4H, s, 3′ 5′), 7.88 (4H, dt, 4 4″), 7.35 (4H, dt, 5 5″), 4.71 (4H, t, CH2), TOF MS-ES^{+}, m/e: 547.1857, $(M + Na)^{+}$.

Bis[4′-(2,2′:6′,2″-terpyridyl)]- diethyleneglycol ether (dtdeg). Yield: 185 mg, (80%), off-white powder. ^{1}H NMR (400 MHz, $CDCl_3$) δ/ppm: 8.69 (4H, d, 6 6″), 8.61 (4H, d, 3 3″), 8.08 (4H, s, 3′ 5′), 7.85 (4H, dt, 4 4″), 7.33 (4H, dt, 5 5″), 4.47 (4H, t, CH2), 4.07 (4H, t, CH2), TOF MS-ES^{+}, m/e: 591.2115, $(M + Na)^{+}$.

Bis[4′-(2,2′:6′,2″-terpyridyl)]- triethyleneglycol ether (dtteg). Yield: 103 mg, (65%), off-white powder. ^{1}H NMR (400 MHz, $CDCl_3$) δ/ppm: 8.69 (4H, d, 6 6″), 8.61 (4H, d, 3 3″), 8.05 (4H, s, 3′ 5′), 7.84 (4H, dt, 4 4″), 7.32 (4H, dt, 5 5″), 4.42 (4H, t, CH2), 3.97 (4H, t, CH2), 3.81 (4H, t, CH2), TOF MS-ES^{+}, m/e: 635.2371, $(M + Na)^{+}$.

Bis[4′-(2,2′:6′,2″-terpyridyl)]- tetraethyleneglycol ether (dttteg). Yield: 98 mg, (67%), off-white powder. ^{1}H NMR (400 MHz, $CDCl_3$) δ/ppm: 8.69 (4H, d, 6 6″), 8.61 (4H, d, 3 3″), 8.05 (4H, s, 3′ 5′), 7.84 (4H, dt, 4 4″), 7.31 (4H, dt, 5 5″), 4.40 (4H, t, CH2), 3.94 (4H, t, CH2), 3.78 (4H, t, CH2), 3.72 (4H, t, CH2), TOF MS-ES^{+}, m/e: 679.2626, $(M + Na)^{+}$.

Synthesis of Pt(II)complexes

Synthesis of 6′,6″-bis(2-pyridyl)-2,2′:4′,4″:2″,2‴-quaterpyridine platinum(II), (Ptdt)

The silver salt $AgSbF_6$ (68.5 mg, 0.200 mmol) was dissolved in acetonitrile (5 mL) and added to a suspension of $[Pt(PhCN)_2Cl_2]$ (99 mg, 0.200 mmol) in acetonitrile (10 mL). The mixture was refluxed overnight under an inert atmosphere, and the resultant precipitate of AgCl was filtered off. An equimolar amount of 6′,6″-bis(2-pyridyl)-2,2′:4′,4″:2″,2‴-quaterpyridine (92.9 mg, 0.200 mmol) was added to the filtrate, and the mixture was refluxed for an additional 24 h. Once the reflux was complete, the mixture was filtered hot and the

solvent partially removed *in vacuo* resulting in the precipitation of [Pt{6′,6″-bis(2-pyridyl)-2,2′:4′,4″:2″,2‴-quaterpyridineCl]SbF_6. The product was washed on the frit with copious amounts of diethyl ether and then smaller amounts of cold acetonitrile. The purity of the complex was confirmed using ^{1}H NMR, ^{195}Pt NMR, elemental analyses, and mass spectroscopy.

Yield: 37 mg, (65%), brown powder. ^{1}H NMR (400 MHz, DMSO) *δ*/ppm: 8.82 (4H, s, 3′ 5′), 8.79 (4H, d, 3 3″), 8.08 (4H, s, 6 6″), 7.85 (4H, dt, 4 4″), 7.33 (4H, dt, 5 5″). ^{195}Pt NMR (DMSO-d_6) ppm: −2710. TOF MS-ES$^+$, m/e: 498.0071, (M^{2+}) ($C_{15}H_{10}Cl_2N_3Pt$ species). Anal. Calcd for $C_{30}H_{20}Cl_4N_6Pt_2{\cdot}2H_2O$: C, 34.90; H, 2.34; N, 8.14. Found: C, 34.44; H, 2.80; N, 7.72.

Synthesis of ethyleneglycol ether linked dinuclear Pt(II) complexes

The synthesis of the complexes was carried out using the following literature procedure [26]: To a stirred solution of [Pt(cod)Cl_2] in dry methanol at room temperature, a suspension of the ligand in dry methanol was added at 65 °C dropwise. The reaction mixture was stirred for 24 h at 45 °C, after which the solution was cooled and filtered. When the bright yellow filtrate was concentrated *in vacuo*, the desired compound was precipitated. The compound was filtered, washed with chloroform (20 mL), cold methanol (1 × 5 mL), diethylether (2 × 15 mL), dried and stored in a desiccator.

The identity and the purity of the final complexes were confirmed using ^{1}H NMR, ^{195}Pt NMR, elemental analyses, and mass spectroscopy. The ^{1}H NMR spectra show similarity in the aromatic region. Presence of a peak at −2500 to −2700 ppm on the ^{195}Pt NMR spectra confirms the coordination of the ligand to platinum.

(Ptdteg). Yield: 35 mg, (45%), red brown powder. ^{1}H NMR (400 MHz, DMSO-d_6) *δ*/ppm: 8.97 (4H, s, 3′ 5′), 8.94 (4H, d, 6 6″), 8.70 (4H, d, 3 3″), 8.55 (4H, dt, 4 4″), 7.99 (4H, dt, 5 5″), 4.71 (4H, t, CH2), ^{195}Pt NMR (DMSO-d_6) ppm: −2714. TOF MS-ES+, m/e: (M^{2+}), 464.1578 ($C_{15}H_{11}ClN_3Pt$ species). Anal. Calcd for $C_{32}H_{24}Cl_4N_6O_2Pt_2$: C, 36.38; H, 2.29; N, 7.95. Found: C, 35.89; H, 2.72; N, 7.51.

(Ptdtdeg). Yield: 47 mg, (51%), orange powder. ^{1}H NMR (400 MHz, DMSO-d_6) *δ*/ppm: 8.57 (4H, d, 6 6″), 8.43 (4H, d, 3 3″), 8.2 (4H, dt, 4 4″), 8.17 (4H, s, 3′ 5′), 7.80 (4H, dt, 5 5″), 4.66 (4H, t, CH2), 4.01 (4H, t, CH2), ^{195}Pt NMR (DMSO-d_6) ppm: −2699. TOF MS-ES+, m/e: 568.1068, (M^{2+}) ($C_{19}H_{18}ClN_3O_3Pt$ species). Anal. Calcd for $C_{34}H_{28}Cl_4N_6O_3Pt_2$: C, 37.10; H, 2.56; N, 7.64. Found: C, 36.78; H, 2.92; N, 7.17.

(Ptdtteg). Yield: 56 mg, (57%), orange powder. ^{1}H NMR (400 MHz, DMSO-d_6) *δ*/ppm: 8.71 (4H, d, 6 6″), 8.60 (4H, t, 4 4″), 8.18 (4H, br, 3 3″), 8.06 (4H, s, 3′ 5′), 7.95 (4H, dt, 5 5″), 4.70 (4H, br, CH2), 4.22 (4H, br, CH2), 4.14 (4H, t, CH2), ^{195}Pt NMR (DMSO-d_6) ppm: −2683. TOF MS-ES+, m/e: 568.1073, (M^{2+}) ($C_{19}H_{18}ClN_3O_3Pt$ species). Anal. Calcd for $C_{36}H_{32}Cl_4N_6O_4Pt_2$: C, 37.77; H, 2.82; N, 7.34. Found: C, 37.38; H, 3.30; N, 6.91.

(Ptdttteg). Yield: 56 mg, (57%), orange powder. ^{1}H NMR (400 MHz, DMSO-d_6) *δ*/ppm: 8.71 (4H, d, 6 6″), 8.61 (4H, t, 4 4″), 8.38 (4H, br, 3 3″), 8.03 (4H, s, 3′ 5′), 7.98 (4H, dt, 5

5″), 4.48 (4H, br, CH2), 4.06 (4H, br, CH2), 4.01 (4H, br, CH2), 4.00 (4H, br, CH2), ^{195}Pt NMR (DMSO-d_6) ppm: −2691. TOF MS-ES$^+$, m/e: 887.2581, (M^{2+}), ($C_{38}H_{36}ClN_6O_5Pt$ species). Anal. Calcd for $C_{38}H_{36}Cl_4N_6O_5{\cdot}7H_2O$: C, 34.02; H, 3.64; N, 6.61; Found: C, 34.49; H, 3.41; N, 6.15.

Details of the characterization data agree well with the proposed chemical structure of the complexes. The ^{1}H NMR spectra of Pt(II) complexes show small shifts in comparison with their free ligands. Representative spectra for analysis are given as supporting information.

Instrumentation and physical measurements

^{1}H NMR and ^{13}C NMR spectra were recorded on either a Bruker Avance DPX 400 or 500 MHz spectrometer at 298 K using $Si(CH_3)_4$ as the reference for chemical shifts. ^{195}Pt NMR were done on a 500 MHz spectrometer (^{195}Pt, 107.5 MHz) chemical shifts externally referenced to $K_2[PtCl_6]$. Low-resolution electron spray ionization (ESI$^+$) mass spectra were recorded on a TOF Micromass spectrometer. Elemental analyses were performed by a Thermal Scientific Flash 2000. Kinetic analyses were studied on an Applied Photophysics SX20 stopped-flow reaction analyzer coupled with an online data acquisition system with controlled temperature within ±0.1 °C. The wavelengths for the kinetic analysis were predetermined on a Varian Cary 100 Bio UV/visible spectrophotometer with an attached Varian Peltier temperature-controller within ±0.1 °C and an online kinetic application.

Computational modeling

Computational modeling for the complexes was performed at density functional theoretical (DFT) level in methanol based on B3LYP [39–41]/LanL2DZ [39, 42–44] Los Alamos National Laboratory 2 double ξ level theory, with inner core electrons of Pt replaced by relative effective core potential (ECP). Due to low electronic spin of Pt(II), the DFT calculations of the complexes were done as singlet states. The complexes were computed in methanol solution taking into account the solvolysis effect by means of the conductor polarizable continum model (CPCM) [45, 46]. The Gaussian09 suite of program was used for all computations [47].

Kinetic analyses

All kinetic measurements were performed under *pseudo*-first-order conditions using at least 20-fold excess (a 10-fold excess of nucleophile at each Pt(II) center) of the nucleophile in 0.02 M ionic solution, made by dissolving the required amount of $LiCF_3SO_3$ (0.018 M) and LiCl (0.002 M) in dry methanol. LiCl was added to suppress any possibility of solvolysis reactions. Since $CF_3SO_3^-$ does not coordinate with the Pt(II) metal center [48], all substitution kinetics were studied in this media. Nucleophiles were used in large excess to drive the reactions to completion.

Pt(II) complex solutions were prepared by dissolving the required amount of the complex in ionic solution. Nucleophile solutions were prepared at 100 times the concentration of the Pt(II) complex. Subsequent dilutions of the nucleophile stock solution afforded solutions of 20, 40, 60, and 80 times that of the metal complex. The wavelengths chosen for the kinetic investigations were pre-determined by monitoring the change in absorbance of the mixture

of the metal complex and the nucleophile as a function of time using UV/visible absorption spectra and are summarized in table S1 (see online supplemental material at http://dx.doi.org/10.1080/00958972.2015.1064114). All data were graphically analyzed using the software package Origin 7.5® [49] to determine the observed rate constants, k_{obs}.

Results

Substitution kinetics of coordinated chlorides from the Pt(II) complexes by thiourea nucleophiles, *viz*. TU, DMTU, and TMTU were investigated under pseudo-first-order conditions using a conventional stopped-flow reaction analyzer. An example of a time-resolved kinetic trace obtained from a stopped-flow analyzer for the simultaneous substitution of the chloride ligands in **Ptdtteg** (3.0×10^{-5} mol dm^{-3}) with DMTU (0.899 mol dm^{-3}) at 298 K is given in figure 2.

All kinetic data obtained were fitted to a first-order exponential decay function to generate the observed *pseudo*-first-order rate constants, (k_{obs}), which were plotted against the concentration of the incoming nucleophiles. The values used represent an average of at least eight independent runs. Straight line graphs with zero intercepts were obtained for each nucleophile, indicating that the reactions were irreversible and can be represented by scheme 1 and the corresponding rate law given by equation (1) [50]. Representative plots for **Ptdteg**, shown in figure 3, clearly indicate that the substitution reactions were first order with respect to the incoming nucleophile. Kinetic data obtained from the slope of equation (1) are summarized in table 1.

$$k_{obs} = k_2[\mathrm{Nu}] \tag{1}$$

The temperature dependence studies were performed in a similar manner using a single nucleophile concentration from 15 to 40 °C in 5 °C intervals. The activation parameters,

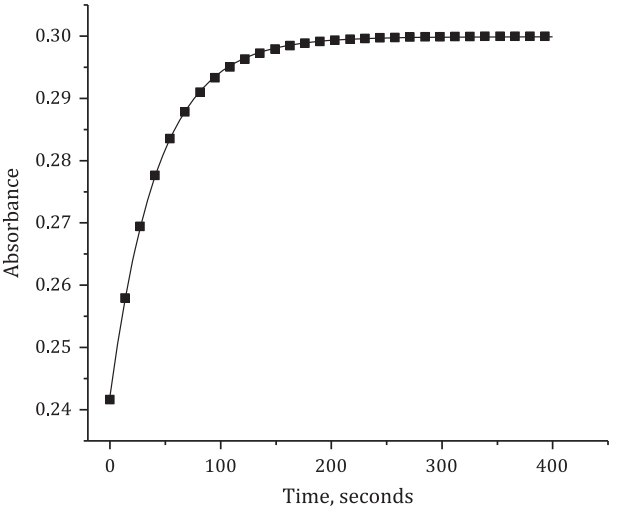

Figure 2. Kinetic trace at 301 nm for the reaction of Ptdtteg (3.0×10^{-5} mol dm^{-3}) with DMTU (8.99×10^{-4} mol dm^{-3}) at 298 K, I = 0.02 M $LiCF_3SO_3$, adjusted with LiCl.

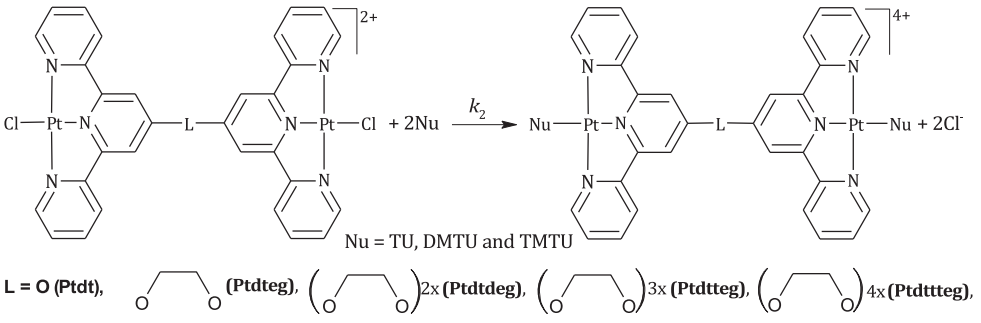

Scheme 1. Proposed substitution mechanism for the dinuclear Pt(II) complex system with thiourea nucleophiles.

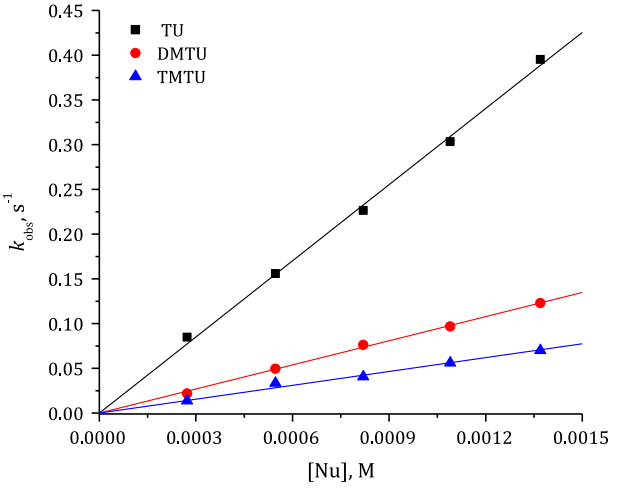

Figure 3. Dependence of the *pseudo*-first-order rate constants (k_{obs}) on the concentrations of the nucleophiles for the chloride substitution from Ptdteg (2.65×10^{-5} M) in methanol solution (I = 0.02 M) at 298 K.

entropy of activation ($\Delta S^{\neq}$), and enthalpy of activation ($\Delta H^{\neq}$) were then obtained using the Eyring equation [50]. Figure 4 shows representative plots obtained for **Ptdteg** with the different nucleophiles for the forward reactions. The data obtained are summarized in table 1.

Computations

The geometry-optimized structures of the platinum complexes investigated and their distribution of electron density are shown in table 2. The computational data obtained are summarized in tables 3 and S3. The geometry around the Pt(II) center is slightly distorted square planar which is typical for Pt(II) terpyridine complexes (table S3) [51, 52]. The mappings of the HOMO are concentrated on the Pt(II) center and the chloride ligands, whereas LUMO orbitals mainly lie on the terpyridine ligands. The π systems of the two terpyridine moieties of the ligand interact with the Pt(II) metal center through the metal d orbitals. This makes the two halves of the complex orient at an angle to each other which decreases with

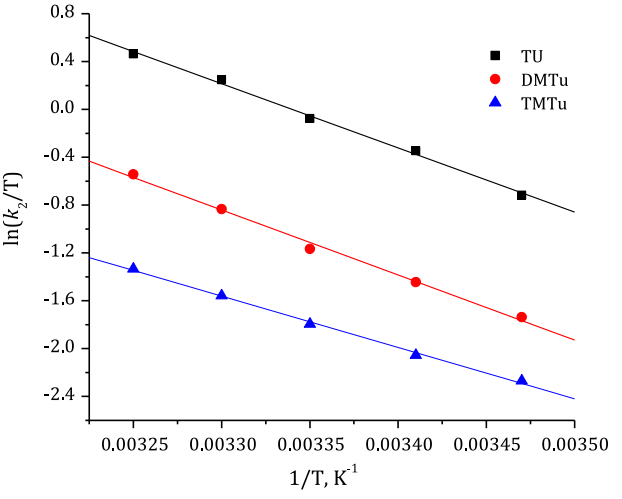

Figure 4. Eyring plots obtained for Ptdteg with the nucleophiles for the forward reactions over the temperature range 15–35 °C.

increase in the length of the linker (δ as represented in figure 5 in **Ptdteg**, **Ptdtdeg,** and **Ptdtteg**). This bonding orientation to platinum prevents possibility of π interaction across the system [53]. As expected, in the back-to-back terpyridine complex, **Ptdt**, the HOMO and LUMO electrons span throughout the molecule due to the extended π conjugation (figure 6, table 2). In the case of the shortest linker (**Ptdteg**), due to the interaction of the lone pair of electrons on O1 with the electrons on the terpyridine ligands [54], the π electron density spreads throughout the ligand system, and hence, the observed DFT-calculated HOMO and LUMO electron density [55]. However, DFT calculations show that the HOMO and LUMO electrons are restricted on one side of the molecules as the length of the spacer between the two terpyridine ligands was increased (figure S1, Supporting Information). This might be because the two Pt(II) terpyridine moieties become independent of each other with increase in the chain length. Furthermore, the two terpyridine moieties lie at an inclined angle, α, which increases with increase in the chain length as exemplified in figure 5.

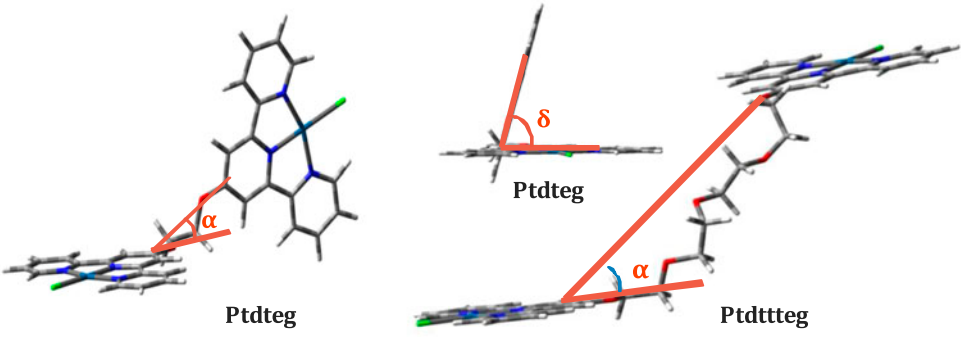

Figure 5. Aerial view showing the angles of inclination, α, in the DFT-calculated distorted slipup stair case like linkers and the angle of twisting of the tpy moieties from each other, δ.

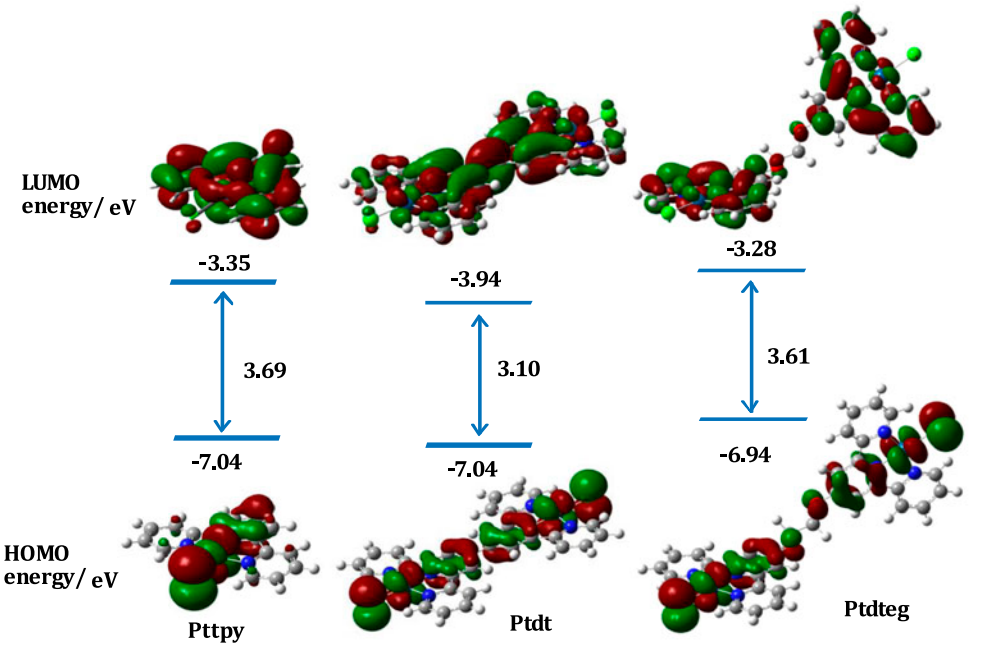

Figure 6. DFT-calculated minimum energy structures, frontier molecular orbitals (HOMO and LUMO) of Pttpy, Ptdt, and Ptdteg. Data for Pttpy are included for comparisons. Data for Ptdtdeg, Ptdtteg, and Ptdttteg are included in figure S1 (Supporting Information).

When comparing the DFT-calculated NBO charges on Pt and N_{trans} of **Pttpy** and back-to-back linked complex, **Ptdt**, the charge on Pt increases from **Pttpy** to **Ptdt** while it decreases for N_{trans} from **Pttpy** to **Ptdt**. However, when comparing from **Ptdt** to **Ptdteg**, the opposite was observed, i.e., the NBO charge on the Pt decreases from **Ptdt** to **Ptdteg** then remains constant, while the opposite is true for N_{trans} which becomes more negative and remains constant as the chain length increases. This observation for **Ptdt** and **Ptdteg** is due to the inductive σ donation from the ethyleneglycol ether linker to Pt(II). Nevertheless, the fact that the values are roughly constant as the length of the polyethyleneglycol ether linker is increased indicates that the σ inductive effect does not play a significant role on increasing the length of the linker beyond one unit of ethyleneglycol ether. Furthermore, since the DFT-based global electrophilicity index (ω, related to the capacity of the molecule to accept electrons) [56–58], obtained using the chemical hardness (η) [59] and electronic potential (μ) [58], is a strong tool to determine the chemical reactivity, this parameter was calculated and the values show similar trend between **Pttpy**, **Ptdt,** and **Ptdteg** as reported above.

Discussion

In this study, substitution kinetics of chloride ligands from the dinuclear Pt(II) complexes by thiourea nucleophiles occurred simultaneously by a single step. Data summarized in tables 1 and 3 show that the Pt(II) complexes are symmetrical such that the nucleophiles

Table 1. Summary of the second-order rate constants, k_2, and activation parameters, with the corresponding standard deviations for the substitution of chloro ligands by a series of thiourea nucleophiles at $I = 0.02$ M $LiCF_3SO_3$, adjusted with LiCl. Data for Pttpy are taken from the literature [51] and included for comparison.

Complex	Nu	k_2 ($M^{-1} s^{-1}$)	$\Delta S^{\neq}$ ($J K^{-1} mol^{-1}$)	$\Delta H^{\neq}$ ($kJ mol^{-1}$)
Pttpy	TU	1494 ± 10	−88 ± 5	28.7 ± 1.5
	DMTU	448 ± 10	−73 ± 4	36.4 ± 1.1
	TMTU	82 ± 4	−91 ± 8	35.0 ± 2.0
Ptdt	TU	1520 ± 28	−85 ± 6	30.0 ± 1.8
	DMTU	838 ± 14	−31 ± 7	47.9 ± 2.2
	TMTU	139 ± 3	−50 ± 8	46.1 ± 2.5
Ptdteg	TU	281 ± 2	−52 ± 6	43.6 ± 1.7
	DMTU	90 ± 1	−59 ± 3	54.3 ± 1.0
	TMTU	52 ± 1	−96 ± 2	35.0 ± 0.7
Ptdtdeg	TU	132 ± 2	−50 ± 3	46.2 ± 1.1
	DMTU	43 ± 0.6	−89 ± 4	37.1 ± 1.1
	TMTU	27 ± 0.2	−88 ± 3	38.8 ± 0.8
Ptdtteg	TU	100 ± 1	−96 ± 5	33.2 ± 1.5
	DMTU	40 ± 0.6	−62 ± 6	45.4 ± 1.8
	TMTU	14 ± 0.2	−49 ± 12	51.2 ± 3.7
Ptdttteg	TU	43 ± 0.7	−49 ± 5	49.3 ± 1.5
	DMTU	28 ± 0.4	−69 ± 6	44.6 ± 1.8
	TMTU	22 ± 0.4	−78 ± 8	42.4 ± 2.3
Ptttpyeg	TU	257 ± 5	−56 ± 6	43 ± 2
	DMTU	81 ± 1	−98 ± 6	33 ± 2
	TMTU	22 ± 1	−57 ± 7	40 ± 2

cannot differentiate the two Pt(II) centers. The symmetrical nature of the Pt(II) centers is supported by the DFT calculated similar NBO charges on Pt(II) (table 3) indicating that the two Pt(II) centers are in similar chemical environments regardless of the distance between the two Pt(II) centers. Similar substitution behavior has been reported previously by Jaganyi and co-workers [60], for dinuclear Pt(II) complexes containing flexible diamine linkers.

Simultaneous substitution of the chloride ligands is further confirmed using ^{195}Pt NMR of **Ptdtteg** with TU (2 eqv) in DMF-d^6 (figure 7). At t = 0, a signal due to the starting complex (**Ptdtteg**) is observed at $\delta = -2687$ ppm, represented as A. This chemical shift at $\delta = -2687$ ppm has moved to $\delta = -3099$ ppm, (B) after 3 h and is attributed to the formation of $[(TU)Pt(Ptdtteg)Pt(TU)]^{4+}$ which exhibits a chemical shift due to Pt(NNNTU) centers as reported by Jaganyi *et al.* [35]. Unlike the previous findings for dinuclear Pt(II) complexes with flexible diamine [31, 33], rigid azine [35], and cyclic [27] linkers, the dinuclear complexes reported in this work are more stable showing no dechelation as can be seen from figure 7.

When compared to the mononuclear analog, **Pttpy** with the linker-free back–to-back terpyridine complex, **Ptdt**, the reactivity increases slightly which can be attributed to the expansion of the π-conjugated electron system over the two Pt(II) centers. This increases the electronic communication within the terpyridine ligand system, decreasing the electron density at the Pt(II) metal center caused by the enhanced π-backbonding ability of the ligand system [61]. Thus, the Pt(II) metal centers in **Ptdt** become more electrophilic, enhancing the binding of the incoming nucleophile. This is clearly seen from the DFT-calculated NBO charges on the Pt ions which increases from **Pttpy** to **Ptdt**. Further support for this comes from the remarkably higher DFT-calculated global electrophilicity index of **Ptdt** compared to **Pttpy**, a clear indication of the greater ability of **Ptdt** to accept electron

Table 2. Geometry-optimized structures of the complexes investigated.

Complex	Complex
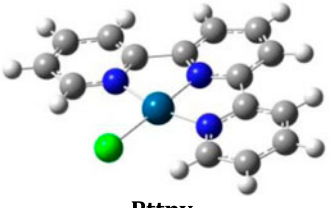 **Pttpy**	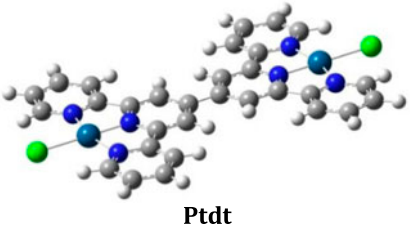 **Ptdt**
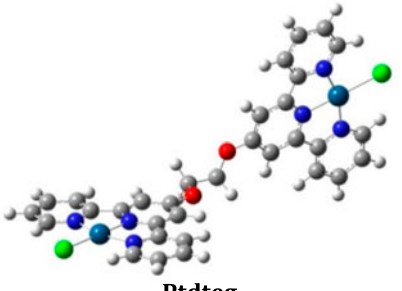 **Ptdteg**	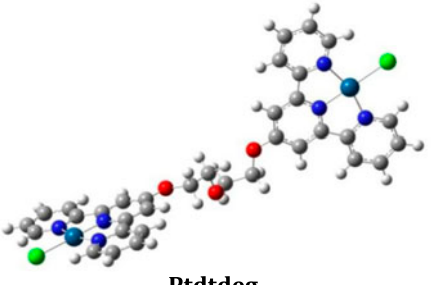 **Ptdtdeg**
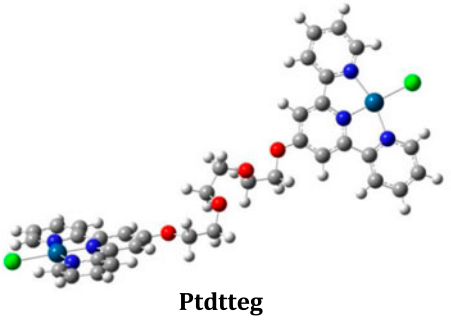 **Ptdtteg**	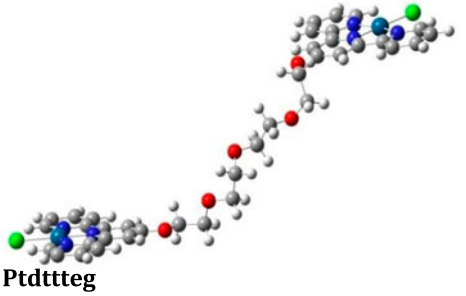 **Ptdttteg**

density from the incoming nucleophile than that of **Pttpy** [57, 58, 62]. The increase in π-backbonding together with the increased overall charge [19, 33] of 2+ attributes to the higher substitution reactivity of **Ptdt**. Compared to **Pttpy** and to the rest of the complexes steric hindrance is an additional factor.

To understand the role of the linker on the rate of substitution of chloride ligands, the reactivity of **Ptdt** and **Ptdteg** is compared to explain the huge drop in the reactivity. The difference between them is the presence of the ethyleneglycol ether linker for **Ptdteg**. The kinetic data show that the reactivity of **Ptdt** is five times greater than **Ptdteg** which implies that as reported in our previous work [63], the ethyleneglycol ether linker acts as a σ donor using the two lone pairs of electrons on O1. This inductive σ donation increases the charge on the N_{trans} from **Ptdt** (−0.446) to **Ptdteg** (−0.469) which in turn decreases the NBO charge on the Pt atom from **Ptdt** (0.620) to **Ptdteg** (0.595). This is in line with the

Table 3. Summary of DFT-calculated data for the complexes investigated. Included are the data obtained for the DFT-calculated Pttpy complex for comparisons.

Complex	Pttpy	Ptdt	Ptdteg	Ptdtdeg	Ptdtteg	Ptdttteg
Bond length (Å)						
Pt—Cl	2.44	2.44	2.44	2.44	2.45	2.44
Pt—N1(trans)	1.96	1.95	1.96	1.96	1.96	2.96
Length of linker	–	–	2.93	5.04	8.32	11.65
Pt···Pt	–	10.95	14.34	16.99	19.95	21.87
Bond angles (°)						
Dihedral angle (δ)	–	3.3	65.5	56.6	56.0	10.6
Inclination angle (α)	–	0.0	20.4	25.8	26.0	45.1
NBO charges						
Pt1/Pt2	0.604	0.620	0.595	0.593	0.593	0.592
N1 (trans)	−0.453	−0.446	−0.469	−0.471	−0.470	−0.471
Cl	−0.502	−0.496	−0.504	−0.504	−0.505	−0.505
ΔE (eV)	3.69	3.10	3.61	3.64	3.64	3.64
η (eV)	1.85	1.55	1.83	1.82	1.82	1.82
μ (eV)	−5.20	−5.49	−5.11	−5.09	−5.08	5.07
ω (eV)	7.31	9.72	7.13	7.12	7.09	7.06
Symmetry	C_2	C_1	C_1	C_1	C_1	C_1

Note: η = chemical hardness, μ = chemical potential, and ω = global electrophilicity index [56–59].

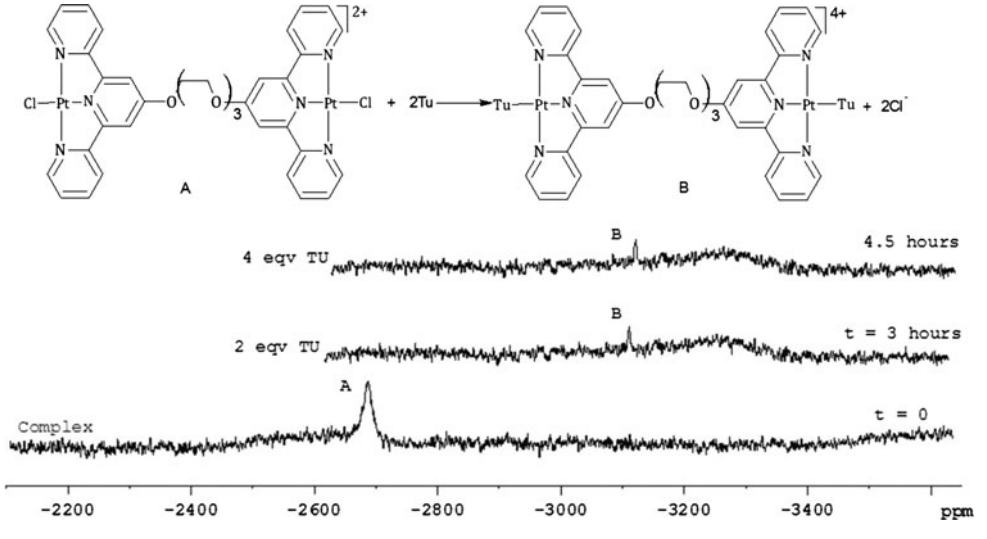

Figure 7. ^{195}Pt NMR spectra for the reaction mixture of Ptdtteg (2×10^{-2} M) with six equivalents of TU (2.0 M), showing a peak for pure dinuclear Pt(II) complex at $\delta = -2687$ ppm before the reaction ($t = 0$) and the final substituted product (B, $\delta = -3099$ ppm) corresponding to $[(TU)Pt(dtteg)Pt(TU)]^{4+}$, over a period of 3 h after the reaction begins.

literatures [3, 51, 64, 65], where electron-donating groups on the ancillary position of terpyridine reduce the positive charge at the metal center, thereby decreasing its electrophilicity. Further support for this comes from the significant decrease in the DFT-calculated global electrophilicity index for **Ptdteg** (7.13 eV) to that of **Ptdt** (9.72 eV). Hence, **Ptdt** has a greater tendency to accept the incoming nucleophiles, and thus enhances the π-backbonding

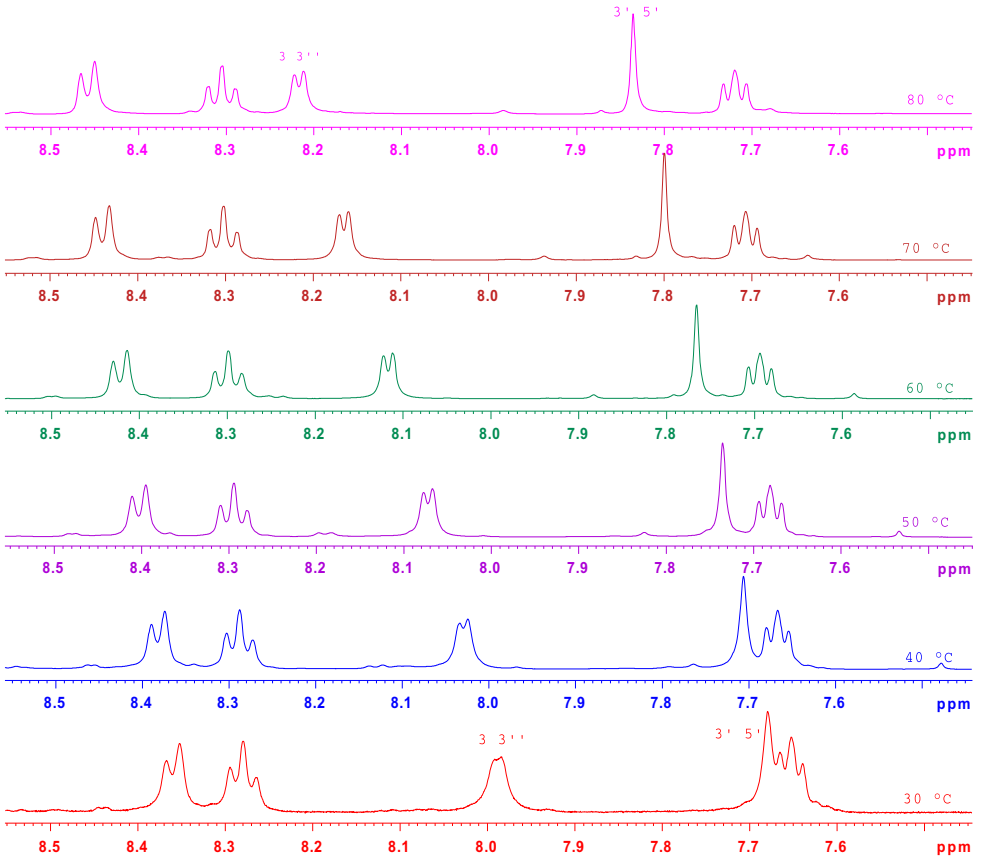

Figure 8. ^{1}H spectra of Ptdttteg (0.02 M) in DMSO-d_6 at 30–80 °C.

of electrons from the Pt d_{xz} orbital into the antibonding π^* orbital whereby stabilizing the transition state intermediate. In other words, the significantly slower reactivity of **Ptdteg** indicates that the nature of the bridging ligand in **Ptdteg** decreases the π-backbonding ability of the terpyridine moiety [61]. Together with the mentioned electronic effects, the decrease in rate of substitution reactions from the linker-free **Ptdt** to **Ptdteg** is also due to the presence of the axially imposed steric influences on one side of the Pt(II) coordination sphere as illustrated in figure 5.

Further analysis of the reactivity of the polyethyleneglycol ether linked complexes shows a decrease in the reactivity as the length of the linker is increased from **Ptdteg** (2.926 Å) to **Ptdettteg** (11.65 Å). When viewed along the axis perpendicular to the mean planes containing the Pt ions, the DFT-calculated minimum energy structures show that the complexes adopt twisted slipup staircase-like geometry so that the second terpyridine lies in an inclination angle, α which is dependent on the length of the linker. Relative to the plane containing one of the terpyridine moieties, the other chelate moiety projected by the linker increases from 20.44° in **Ptdteg** to 45.14° in **Ptdttteg**. Thus, the steric imposition on one side of the Pt(II) coordination sphere increases with increase in the length of the linker, impeding the

approach of the axially incoming nucleophile. This steric influence is the main factor responsible for the decreasing reactivity from **Ptdteg** to **Ptdttteg**. This deduction is also supported when one compares the reactivity trend of these dinuclear complexes to that of mononuclear complexes which shows the reactivity to be relatively constant as the linker is increased [63]. This trend in the decrease in the reactivity has been reported by van Eldik *et al.* [25, 32] and Jaganyi *et al.* [60] for dinuclear Pt(II) complexes with flexible linkers.

In addition to steric hindrance, the decrease in reactivity is also attributed to the fact that the charges on the metal centers do not affect each other [25, 66–68], thus reducing the overall electrophilicity of the molecule as supported by the DFT calculation [58]. It can also be argued that the other factor contributing to the observed decrease in the reactivity from **Ptdteg** to **Ptdttteg** is increased in electrostatic attraction induced between the ethyleneglycol ether polymer units and the Pt centers and the terpyridine moieties by the lone pair of electrons on oxygen in the linker [69].

To further investigate the steric influence introduced by the linker, analysis of ^{1}H NMR study of **Ptdttteg** (0.02 M) at six different temperatures (30–80 °C, figure 8, also see figure S26, Supporting Information) shows more downfield chemical shifts with improved multiplicity (in case of proton 3 3″ from broad to a doublet) with increase in the temperature. This is an indication of the disruption of the self-associated dimers such as π stacked molecules in solution at high temperature [70]. However, since the kinetic investigations are performed at 10^{-5} M, in such diluted solution, the probability of formation of dimers is unlikely. Therefore, the improved multiplicity is due to the relief of intrinsic steric effect within the complex which is due to the increase in rotations about the flexible linker. This increases with the increase in the length of the linker which imposes a greater degree of steric influence on the Pt(II) center. This has a net effect of influencing the axial attack of the incoming nucleophile, slowing the reactivity [60].

In general, when comparing the reactivity of the Pt(II) dinuclear complexes with their representative monomer, the reactivity of the dinuclear complexes was slower than the reactivity of the mononuclear complexes. Unlike the mononuclear complexes, the reactivity of the dinuclear complexes decreases with increase in the length of the linker. However, one notes that the reactivity of the Pt(II) dinuclear complex with the shortest linker **Ptdteg** is slightly faster (281 ± 2 M^{-1} s^{-1}) than its monomer, **Pttpyeg** (257 ± 5 M^{-1} s^{-1}) (see table S14). We believe that this increase in the reactivity is related to the increased overall charge of the molecule; when the distance between the two Pt(II) centers is small, the molecule behaves more like a 2 + charge at each metal center than 1+ [25]. The current observation is contrary to other dinuclear complexes with flexible linkers that we have investigated which showed an increase in reactivity with increase in the linker chain [33, 71], *i.e.,* reduction in steric hindrance. This difference is due to change in the angle of inclination/elevation (α). In the case of ethyleneglycol, this angle increases resulting in one side of the metal center being hindered, unlike in alkanediamine, the angle decreases opening the entry for the incoming nucleophile.

The reactivity of the nucleophiles shows a clear dependence on steric effects, which is typical of a mechanism involving bond making in the transition state [27, 31]. In all cases, TU has the highest reactivity and the rate decreases as the incoming nucleophile gets bulky, *i.e.*, rate with TMTU is significantly slower. The large entropies of activation ($\Delta S^{\neq}$) suggest a more ordered transition state. The relatively small enthalpies of activation ($\Delta H^{\neq}$) support an easy bond formation in the transition state which is typical for d^8 square planar Pt(II) complexes with associative mode of substitution [33, 35, 51, 52, 65, 72–74].

Conclusion

The lability of the dinuclear polyethyleneglycol ether linked complexes **Ptdteg**, **Ptdtdeg**, **Ptdtteg,** and **Ptdttteg** differs significantly from the corresponding linker-free dinuclear complex, **Ptdt**, and the monomeric complex, **Pttpy**. The differences in reactivity can be accounted for in terms of the electronic as well as steric effect due to structural differences. The introduction of the linker results in decreased electrophilicity of the platinum center and the whole complex because the ethyleneglycol ether acts as a σ donor using the lone pair of electrons on oxygen. In addition, the reactivity of the ethyleneglycol ether linked complexes decreases with increase in the distance between the Pt(II) metal centers. This is due to steric hindrance which increases with the length of the linker. Unlike the mononuclear Pt(II) complexes whose reactivity remains relatively constant [63], the reactivity of these dinuclear complexes decreases with increase in the length of the linker [33, 71]. The trend also differs from the other flexible linkers such as alkanediamine. This difference is due to the increase in the angle of inclination between the two metal centers in this study compared to a decrease in the case of alkanediamine.

The substitution reactions of these complexes have shown to be more stable with the S-donor nucleophiles compared to what has been reported in the literature which showed dechelation of the ligand and linker [27, 33, 35]. The substitution rates showed a positive dependence to the steric effects of the incoming nucleophiles; hence, the rate constants for TU are much faster than DMTU and TMTU. The activation parameters, enthalpy of activation, and entropy of activation support an associative mechanism. This study clearly shows that the nature of the bridging ligand influences the rate of substitution reactions when compared to the similar studies reported in the literature [25, 33].

Acknowledgements

The authors greatly acknowledge the financial support to Aishath Shaira from the University of KwaZulu-Natal, South Africa. We also thank Mr Craig Grimmer for his support with NMR measurements and Mrs Janse van Resenburg for her help with mass spectra and elemental analysis.

Disclosure statement

No potential conflict of interest was reported by the authors.

References

[1] T. Storr, K.H. Thompson, C. Orvig. *Chem. Soc. Rev.*, **35**, 534 (2006).
[2] J. Reedijk. *Proc. Natl. Acad. Sci. USA.*, **100**, 3611 (2003).
[3] E. Pantoja, A. Gallipoli, S. van Zutphen, S. Komeda, D. Reddy, D. Jaganyi, M. Lutz, D.M. Tooke, A.L. Spek, C. Navarro-Ranninger, J. Reedijk. *J. Inorg. Biochem.*, **100**, 1955 (2006).
[4] E. Wong, C.M. Giandomenico. *Chem. Rev.*, **99**, 2451 (1999).
[5] S. Roy, J.A. Westmaas, K.D. Hagen, G.P. van Wezel, J. Reedijk. *J. Inorg. Biochem.*, **103**, 1288 (2009).
[6] N.J. Wheate, J.G. Collins. *Coord. Chem. Rev.*, **241**, 133 (2003).
[7] V. Brabec, J. Kasparkova. *J. Drug Resist. Updates*, **8**, 131 (2005).
[8] M.J. Bloemink, J. Reedijk. *Met. Ions Biol. Syst.*, **32**, 641 (1996).

[9] M. Adams, AH Calvert, J Carmichael, PI Clark, RE Coleman, HM Earl. *Br. J. Cancer*, **78**, 1404 (1998).
[10] S. Komeda, M. Lutz, A.L. Spek, M. Chikuma, J. Reedijk. *Inorg. Chem.*, **39**, 4230 (2000).
[11] N. Farrell, S.G. De Almeida, K.A. Skov. *J. Am. Chem. Soc.*, **110**, 5018 (1988).
[12] N. Farrell, Y. Qu, M.P. Hacker. *J. Med. Chem.*, **33**, 2179 (1990).
[13] S. Komeda, M. Lutz, A.L. Spek, Y. Yamanaka, T. Sato, M. Chikuma, J. Reedijk. *J. Am. Chem. Soc.*, **124**, 4738 (2002).
[14] N. Summa, J. Maigut, R. Puchta, R. van Eldik. *Inorg. Chem.*, **46**, 2094 (2007).
[15] Q. Liu, Y. Qu, R. van Antwerpen, N. Farrell. *Biochemistry*, **45**, 4248 (2006).
[16] N. Farrell. *Comments Inorg. Chem.*, **16**, 373 (1995).
[17] J. Kasparkova, J. Zehnulova, N. Farrell, V. Brabec. *J. Biol. Chem.*, **277**, 48076 (2002).
[18] N.P. Farrell, S.G. De Almeida, K.A. Skov. *J. Am. Chem. Soc.*, **110**, 5018 (1988).
[19] M.S. Davies, D.S. Thomas, A. Hegmans, S.J. Berners-Price, N. Farrell. *Inorg. Chem.*, **41**, 1101 (2002).
[20] Y. Qu, N.J. Scarsdale, M.C. Tran, N. Farrell. *J. Inorg. Biochem.*, **98**, 1585 (2004).
[21] S.W. Johnson, K.V. Ferry, T.C. Hamilton. *Drug Resist. Updates*, **1**, 243 (1998).
[22] M.S. Davies, J.W. Cox, S. Berners-Price, W. Barklage, Y. Qu, N. Farrell. *Inorg. Chem.*, **39**, 1710 (2000).
[23] Y. Qu, N. Farrell. *J. Am. Chem. Soc.*, **113**, 4851 (1991).
[24] R.A. Kortes, S.J. Geib, F.-T. Lin, R.E. Shepherd. *Inorg. Chem.*, **38**, 5045 (1999).
[25] A. Hofmann, R. van Eldik. *J. Chem. Soc., Dalton Trans.*, **15**, 2979, (2003).
[26] S. Roy. Synergy of intercalation and coordination binding to design novel DNA-targeting antineoplastic metallodrugs. PhD thesis, University of Leiden (2008), pp. 230–248.
[27] A. Mambanda, D. Jaganyi. *Dalton Trans.*, **41**, 908 (2012).
[28] G.V. Kalayda. F.d.W.e. Natuurwetenschappen (Ed.), Dinuclear platinum complexes as potential anticancer drugs: insight in the intercellular distribution. PhD thesis, University of Leiden (2006), pp. 125-137.
[29] J. Kasparková, O. Vraná, N. Farrell, V. Brabec. *J. Biol. Inorg. Chem.*, **98**, 1560 (2004).
[30] W.D. McFadyen, L.P.G. Wakelin, I.A.G. Roos, V.A. Leopold. *J. Med. Chem.*, **28**, 1113 (1985).
[31] H. Ertürk, J. Maigut, R. Puchta, R. van Eldik. *J. Chem. Soc., Dalton Trans.*, **20**, 2759, (2008).
[32] H. Ertürk, A. Hofmann, R. Puchta, R. van Eldik. *Dalton Trans.*, **22**, 2295 (2007).
[33] D. Jaganyi, A. Mambanda, S. Hochreuther, R. van Eldik. *Dalton Trans.*, **39**, 3595 (2010).
[34] D. Reddy, D. Jaganyi. *Int. J. Chem. Kinet.*, **43**, 161 (2011).
[35] P.O. Ongoma, D. Jaganyi. *Dalton Trans.*, **42**, 2724 (2013).
[36] D.D. Perrin, W.L.F. Armarego, D.R. Perrin. *Purifiction of Laboratory Chemicals*, 2nd Edn, Pergamon, Oxford (1980).
[37] E.C. Constable, M.D. Ward. *J. Chem. Soc., Dalton Trans.*, **4**, 1405, (1990).
[38] K. van der Schilden. The development of polynuclear ruthenium and platinum polypyridyl complexes in search of new anticancer agents. PhD thesis, Laiden University (2006).
[39] A.D. Becke. *J. Chem. Phys.*, **98**, 5648 (1993).
[40] C. Lee, W. Yang, R.G. Parr. *Phys. Rev. B*, **37**, 785 (1988).
[41] P. Stephens, F. Devlin, C. Chabalowski, M.J. Frisch. *J. Phys. Chem.*, **98**, 11623 (1994).
[42] P.J. Hay, W.R. Wadt. *J. Chem. Phys.*, **82**, 270 (1985).
[43] W.R. Wadt, P.J. Hay. *J. Chem. Phys.*, **82**, 284 (1985).
[44] P.J. Hay, W.R. Wadt. *J. Chem. Phys.*, **82**, 299 (1985).
[45] V. Barone, M. Cossi. *J. Phys. Chem. A*, **102**, 1995 (1998).
[46] M. Cossi, N. Rega, G. Scalmani, V. Barone. *J. Comput. Chem.*, **24**, 669 (2003).
[47] M.J. Frisch, G.W. Trucks, H.B. Schlegel, G.E. Scuseria, M.A. Robb, J.R. Cheeseman, G. Scalmani, V. Barone, B. Mennucci, G.A. Petersson, H. Nakatsuji, M. Caricato, X. Li, H.P. Hratchian, A.F. Izmaylov, J. Bloino, G. Zheng, J.L. Sonnenberg, M. Hada, M. Ehara, K. Toyota, R. Fukuda, J. Hasegawa, M. Ishida, T. Nakajima, Y. Honda, O. Kitao, H. Nakai, T. Vreven, J.A. Montgomery, J.E. Peralta Jr., F. Ogliaro, M. Bearpark, J.J. Heyd, E. Brothers, K.N. Kudin, V.N. Staroverov, R. Kobayashi, J. Normand, K. Raghavachari, A. Rendell, J.C. Burant, S.S. Iyengar, J. Tomasi, M. Cossi, N. Rega, J.M. Millam, M. Klene, J.E. Knox, J.B. Cross, V. Bakken, C. Adamo, J. Jaramillo, R. Gomperts, R.E. Stratmann, O. Yazyev, A.J. Austin, R. Cammi, C. Pomelli, J.W. Ochterski, R.L. Martin, K. Morokuma, V.G. Zakrzewski, G.A. Voth, P. Salvador, J.J. Dannenberg, S. Dapprich, A.D. Daniels, O. Farkas, J.B. Foresman, J.V. Ortiz, J. Cioslowski, D.J. Fox, in: I. Gaussian, Wallingford CT, 2009. (Ed.), Gaussian, Inc., Wallingford, CT (2009).
[48] T.G. Appleton, J.R. Hall, S.F. Ralph, C.S.M. Thompson. *Inorg. Chem.*, **23**, 3521 (1984).
[49] Microcal™ Origin™ Version 7.5. Microcal Software, Inc., Northampton, MA (1991-2003).
[50] J.D. Atwood, *Inorganic and Organic Reaction Mechanisms*, 2nd Edn, Wiley-VCH Inc., New York (1997). 32-34, 43-61.
[51] D. Jaganyi, D. Reddy, J.A. Gertenbach, A. Hofmann, R. van Eldik. *Dalton Trans.*, **2**, 299 (2004).
[52] D. Jaganyi, K.L. Boer, J. Gertenbach. *J. Perils. Int. J. Chem. Kinet.*, **40**, 808 (2008).
[53] T.M. Perrine, B.D. Dunietz. *J. Phys Chem. A*, **112**, 2043 (2008).
[54] H.S. Chow. Metal Complexes of 4'-Substituted-2,2′:6′,2″-Terpyridines in Supramolecular Chemistry, China, PhD thesis, University of Basel, (2005). pp. 33–66.

[55] MOE (Molecular Operating Environment). Chemical Computing Group Inc. & Ryoka Systems Inc. Quebec, Canada & Tokyo, Japan (2014).
[56] R.G. Parr, L. Szentpály, S. Liu. *J. Am. Chem. Soc.*, **121**, 1922 (1999).
[57] M. Elango, R. Parthasarathi, G.K. Narayanan, A.M. Sabeelullah, U. Sarkar, N.S. Venkatasubramaniyan, V. Subramanian, P.K. Chattaraj. *J. Chem. Sci.*, **117**, 61 (2005).
[58] C.A. Mebi. *J. Chem. Sci.*, **123**, 727 (2011).
[59] P.K. Chattaraj, U. Sarkar. arXiv:physics/0509089 (2005), 1–38.
[60] D. Jaganyi, V.M. Munisamy, D. Reddy. *Int. J. Chem. Kinet.*, **38**, 202 (2006).
[61] T. Soldatović, S. Jovanović, Živadin D. Bugarčić, R. van Eldik. *Dalton Trans.*, **41**, 876 (2012).
[62] P.K. Chattaraj, S. Giri, S. Duley. *Chem. Rev.*, **111**, PR43 (2011).
[63] A. Shaira, D. Jaganyi. *J. Coord. Chem.*, **67**, 2843 (2014).
[64] A. Hofmann, L. Dahlenburg, R. van Eldik. *Inorg. Chem.*, **42**, 6528 (2003).
[65] D. Reddy, D. Jaganyi. *Dalton Trans.*, **47**, 6724 (2008).
[66] R.A. Ruhayel, J.S. Langner, M.-J. Oke, S.J. Berners-Price, I. Zgani, N.P. Farrell. *J. Am. Chem. Soc.*, **134**, 7135 (2012).
[67] M.S. Davies, J.W. Cox, S.J. Bernenrs-Price, W. Barklage, Y. Qu, N. Farrell. *Inorg. Chem.*, **39**, 1710 (2006).
[68] S. Hochreuther, R. Puchta, R. van Eldik. *Inorg. Chem.*, **50**, 8984 (2011).
[69] C. Yu, K.H.-Y. Chan, K.M.-C. Wong, V.W.-W. Yam. *Chem. Eur. J.*, **14**, 4577 (2008).
[70] V.W.-W. Yam, K.H.-Y. Chan, K.M.-C. Wong, B.W.-K. Chu. *Angew. Chem. Int. Ed.*, **45**, 6169 (2006).
[71] G. Enos, A. Mambanda, D. Jaganyi. *J. Coord. Chem.*, **66**, 4280 (2013).
[72] A. Mambanda, D. Jaganyi. *Dalton Trans.*, **40**, 79 (2011).
[73] S. Ašperger. *Chemical Kinetics and Inorganic Reaction Mechanisms*, 2nd Edn, pp. 152–153, Kluwer Academic/Plenum Publisher, New York, NY (2003).
[74] R. Romeo, M.R. Plutino, L.M. Monsù Scolaro, S. Stoccoro, G. Minghetti. *Inorg. Chem.*, **39**, 4749 (2000).